Cite this article
Afzalimehr H, Barahimi M and Sui J (2019)
Non-uniform flow over cobble bed with submerged vegetation strip.
Proceedings of the Institution of Civil Engineers – Water Management **172(2)**: 86–101,
https://doi.org/10.1680/jwama.17.00039

Research Article
Paper 1700039
Received 20/05/2017;
Accepted 03/11/2017;
Published online 20/12/2017

Keywords: hydraulics & hydrodynamics/ river engineering/waterways & canals

Water Management

ICE Publishing

Non-uniform flow over cobble bed with submerged vegetation strip

1 **Hossein Afzalimehr** PhD
Professor, Department of Civil Engineering, Iran University of Science and Technology, Tehran, Iran

2 **Mahboobeh Barahimi** MS
Former graduate student, Department of Water Engineering, Isfahan University of Technology, Isfahan, Iran

3 **Jueyi Sui** PhD
Professor, Environmental Engineering Program, University of Northern British Columbia, Prince George, BC, Canada (corresponding author: jueyi.sui@unbc.ca)



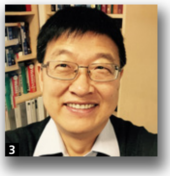

To better understand the influence of non-uniform flow in coarse-bed streams with a submerged vegetation strip on flow characteristics, data were collected from experiments in a laboratory flume and field investigations in a cobble-bed river reach in central Iran. The results of the experiments and field observations showed that the velocity profiles for non-uniform flows in cobble-bed streams with vegetation strips can be divided into either two or three sub-zones. The velocity profiles of non-uniform flows in the laboratory flume and cobble-bed stream deviated from the log law in the wake and mixing zones, but fitted approximately in the log-law layer zone. The distribution of Reynolds stress for non-uniform flows was influenced by the vegetation strip and showed a non-concave shape. Near the channel bed, sweep motion occurred more frequently than the ejection process. Close to the top of vegetation strip, the correlation coefficient ($r_{u'w'}$) was negative, indicating downward momentum transport due to sweep and ejection processes. However, $r_{u'w'}$ was positive near the water surface, indicating upward momentum by the vegetation strip due to inward and outward interactions. The study shows that laboratory results cannot be easily applied to natural rivers without considerable assumptions.

Notation

A	projected plant area perpendicular to flow
$\overline{A_i}$	mean frontal vegetal area
a	vegetation density
d	zero plane displacement
d_{16}	16% finer particle diameters
d_{50}	median grain size
d_{84}	84% finer particle diameters
H	water depth
H'	hole size parameter
h	vegetation bending height
I	detection function
L	length of channel
Q	maximum discharge capacity
Re	Reynolds number
r	correlation coefficient
S	contribution of each event
S_0	bed slope
T	time interval
u	time-averaged velocity in longitudinal direction
u'	velocity fluctuation in longitudinal direction
u_*	shear velocity
u_{i}	instantaneous velocity in longitudinal direction
$u_{\max}$	maximum velocity
u_{rms}	root mean square of stream-wise velocity component
V	vegetation volume
v'	velocity fluctuation in lateral direction
W	channel width
W/H	aspect ratio
w	time-averaged velocity in vertical direction
w'	velocity fluctuation in vertical direction
w_{i}	instantaneous velocity in vertical directions
w_{rms}	root mean square of vertical velocity component
z	distance from bed
z_0	roughness height
β	dimensionless longitudinal pressure gradient
γ	specific gravity of water
κ	von Karman constant
λ	dimensionless vegetation density
ρ	mass density of water
τ	Reynolds stress
τ_0	bed shear stress
σ_{g}	geometric standard deviation
$\partial H/\partial x$	flow depth variation along flume
$\partial p/\partial x$	pressure gradient in longitudinal direction

1. Introduction

Flows in natural streams are rarely uniform due to changes in hydraulic and geomorphological parameters, and non-uniform flows over gravel and cobble beds in the presence of vegetation are frequently observed in natural streams (Afzalimehr *et al.*, 2010; Dey, 2014; Fazel *et al.*, 2015; Fazlollahi *et al.*, 2015; Graf and Altinakar, 1993, 1998). The study reported here was conducted to investigate non-uniform flow with a favourable pressure gradient (FPG) in which the flow depth decreases and the flow velocity increases in longitudinal direction. This kind of non-uniform flow with a FPG is frequently observed over bed forms in natural rivers. However, it is unclear whether or not the reported results hold when a vegetated strip is present along a river reach with a cobble bed. In addition, existing knowledge regarding the interaction between cobbles and vegetation at intermediate relative submergence ($2 < H/d_{50} < 4$) is limited.

It has been reported that velocity profiles in flows with submerged vegetation contain an inflection point near the top of the vegetation (Aberle and Järvelä, 2015; Huai *et al.*, 2008; Kubrak *et al.*, 2015; Lopez and Garcia, 2001). This means that Kelvin–Helmholtz instability exists and induces large-scale vortices (Finnigan, 2000; Raupach *et al.*, 1996). The presence of these vortices dominates momentum exchange and affects turbulence characteristics (Finnigan, 2000; Okamoto and Nezu, 2009).

A better understanding of the changes in the characteristics of non-uniform flow would help the design and development of water resources and environmental engineering projects. Regarding the characteristics of non-uniform flows, much research has been carried out through both experimental laboratory investigations (e.g. Graf and Altinakar, 1998) and theoretical studies (e.g. Franca and Brocchini, 2015). However, research into the interaction between vegetation strips near river banks and cobble beds is very limited. As reported by Choi and Kang (2006), information on partly vegetated open-channel flow is also very limited for streams with other bed conditions. However, all the reported studies indicate that flows over gravel-bed channels with vegetated banks have strong non-homogenous flow profiles.

Afzalimehr (2010) reported that velocity distributions for flow with a FPG over cobble-bed streams have large gradients near the channel bed. At a distance $z/H > 0{\cdot}4$ from the channel bed (z being the distance from the bed and H the flow depth), velocity profiles were shown to be approximately a vertical line towards the water surface.

For flow over a mobile bed, Dey and Das (2012) found that the Reynolds stress from the crest of the bed form to the water surface has a linear distribution. In fact, a linear distribution of Reynolds stress had already been reported by Graf and Altinakar (1998), but over fixed gravel-bed channels. Maddahi *et al.* (2016) investigated flow characteristics over a gravel bed in a river and found more complicated patterns regarding the Reynolds stress and turbulence intensity distributions.

For quasi-uniform flow over a cobble channel bed with vegetated banks, Afzalimehr *et al.* (2014) found that the secondary currents generated by the anisotropy of turbulence caused a change in the shape of the velocity distribution at different distances from the vegetated bank. They found that, near the vegetated bank, the Reynolds stress had a Z-shaped distribution without any negative values. However, along the central axis of the flume and near the water surface, negative values of Reynolds stress were observed in the outer region ($z/H > 0{\cdot}4$). Near the cobble bed, Reynolds stress was found to be positive and sweep events were dominant, followed by ejection processes. However, where the Reynolds stress was negative, the inward and outward interactions were the dominant events, playing more important roles in the Reynolds stress distribution than sweep or ejection processes.

Using the method of quadrant analysis, Fazel *et al.* (2015) studied FPG flows over a gravel-bed flume with vegetated banks. They found that the contributions caused by sweeps and ejections near the gravel bed were more important than those of the outward and inward interactions at the central axis of the flume. They claimed that the stress fraction received a greater contribution from sweep and ejection close to the vegetated walls, revealing no negative values of Reynolds stress near the water surface and close to the vegetated walls.

In the work reported in this paper, the characteristics of turbulent flow in the presence of a submerged vegetation strip under different flow conditions were investigated. Experiments were carried out in the laboratory under conditions of both uniform flow and non-uniform flow with a FPG. Field measurements were also conducted to further investigate the characteristics of turbulent flow along a river reach with a submerged vegetation strip. The data collected from both the laboratory experiments and the field measurements were used to study velocity profiles, Reynolds shear stresses, secondary currents, vorticity parameters, momentum and mass transport. The objective of the work was to study the interaction of non-uniform flow with a cobble bed and a vegetation strip in both a laboratory flume and a river reach. To the best of the authors' knowledge, no other study has been reported for similar conditions. A non-linear distribution of Reynolds stress and an inflection point at the crest of vegetation, showing the effect of Kelvin–Helmholtz instability, was observed in the velocity distributions.

2. Laboratory experiments and field measurements

The experiments were carried out in an 8 m long, 0·4 m wide and 0·6 m deep flume at the Hydraulics Laboratory of Isfahan University of Technology, Iran. Flowing water was supplied by a circulation system with a maximum discharge capacity of 50 l/s. In order to approach the geomorphological conditions of rivers in the field qualitatively, cobble particles were collected from the Kaj River in central Iran and used in the laboratory flume. The experimental setup was not aimed to mimic any particular real situation of natural rivers, so scaling analysis was not necessary. The channel width and water depth of the selected river reach of the Kaj River were 8 m and 28 cm, respectively. According to the theorem of geometric similarity, if the river had been modelled in the laboratory, the particles would be sand size and the water depth 0·6 cm; as a result, the turbulent flow in the Kaj River would have turned into laminar sheet flow unless a geometric distorted model was used (i.e. vertical scale is larger than the horizontal scale). However, geometric distorted models need to be assessed for validity because flow behaviours in a laboratory flume will be different from those in a real river.

The median grain size of the cobble, determined by the Wolman method (Wolman, 1954), was $d_{50} = 52{\cdot}5$ mm and the geometric standard deviation ($\sigma_g = (d_{84}/d_{16})^{0{\cdot}5}$) of the particle size distribution was 1·18 (d_{84} and d_{16} are 84% and 16% finer particle diameters, respectively). Smaller particles of gravel were used to fill the space between cobbles. The bed slope was fixed by varying the thickness of the cobble and gravel layer along the flume to produce a slope of −1·5% along the 8 m long flume. The minimum thickness of the layer was 3 cm at the flume entrance and the maximum thickness was 14·5 cm at the end of the flume near the tailgate. The negative bottom slope and the horizontal water surface led to a decreasing flow depth and increasing flow velocity, generating a non-uniform flow with a FPG (accelerating flow).

In the selected study reach of the Kaj River, the cobble–gravel bed had a median grain size of 37·3 mm and a geometric standard deviation of the bed material of 2·2, with a non-uniform distribution of particles. Figure 1 shows the grain size distributions of the bed material in the river reach and the laboratory flume.

The criterion proposed by Graf and Altinakar (1993, 1998) was used to parameterise flow non-uniformity. Based on this

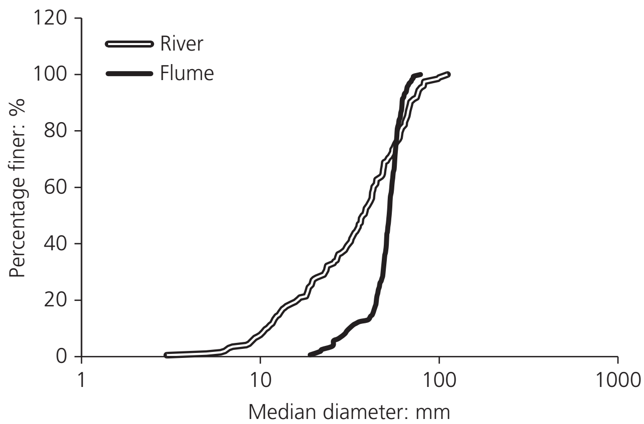

Figure 1. Grain size distribution in the flume and river

criterion, the dimensionless longitudinal pressure gradient parameter (β) is defined as

1. $$\beta = \frac{H}{\tau_0}\frac{\partial p}{\partial x} = \frac{H}{\tau_0}\left[\gamma\left(-S_0 + \frac{\partial H}{\partial x}\right)\right]$$

where H is the flow depth, τ_0 is the bed shear stress, $\partial p/\partial x$ is the pressure gradient in the longitudinal direction, γ is the specific gravity of water, S_0 is the bed slope and $\partial H/\partial x$ is the flow depth variation along the flume.

If it is necessary to change the flow over the measuring test section, keeping all other parameters fixed, equilibrium flow must be produced in the laboratory. This kind of flow requires that β is constant along the test section. In turn, this condition requires that all turbulent flow parameters reveal self-similar distributions in the test section. Equation 1 contains the flow depth gradient, which is extremely difficult to determine. Mrokowska *et al.* (2015a, 2015b) recently discussed this issue and claimed it was highly sensitive to the method used for computations. In this study, to calculate β, the variation in water depth along the flow direction ($\partial H/\partial x$) was determined from the continuous water surface profile, adjusted by a spline fitting technique to the flow depth measurements. Velocity profiles were acquired along the centreline of the flume, with each velocity profile consisting of 20 point velocities. Fluctuating turbulence near the channel bed is more important than that at the water surface. Thus, for the measurements of point velocities, the vertical spacing (i.e. the vertical distance between two consecutive points for measuring the point velocity) was chosen as 2 mm, 5 mm and 10 mm from the vicinity of the channel bed to the water surface. For the case of uniform flow, fully developed flow occurred at a distance 4·5 m downstream from the flume entrance with a water depth of $H = 0{\cdot}2$ m.

To prove that uniform flow is fully developed, the velocity profiles have to be self-similar at different distances from the flume entrance. It was observed that, beyond 4·5 m from the flume entrance, the measured velocity profiles were self-similar (coinciding with each other). Figure 2 shows the fully developed flow condition in this study. Cross-sections at 5·5 m, 6 m, 6·5 m and 6·75 m downstream from the flume entrance were thus chosen for the measurements, as shown in Table 1.

A tail-gate was installed at the end of the flume to maintain a flow depth of 0·2 m. A grid wall was set at the flume inlet to prevent additional confusion caused by the flowing water entering the flume from the source.

In the laboratory flume, to investigate the impacts of vegetation along the channel bank on the turbulence characteristics, grassy weeds with long leaves were collected from the Kaj River and embedded in the gaps between cobbles along a longitudinal line (parallel to the flume wall) at a distance of 13 cm from the flume wall (Figure 3). Although setting up the

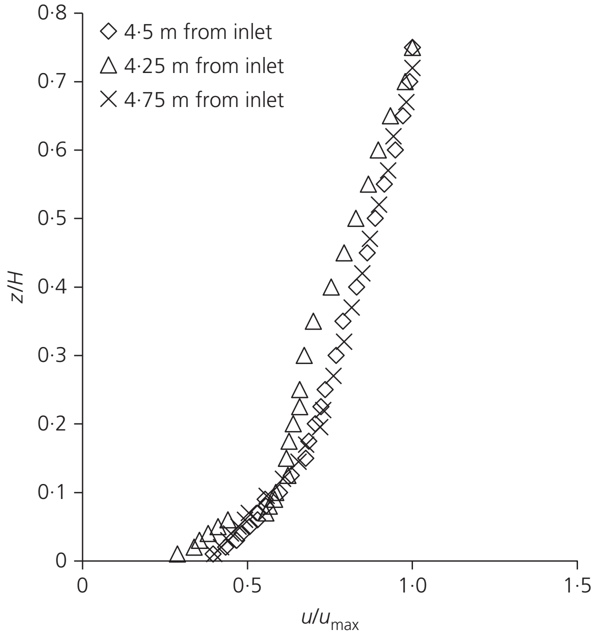

Figure 2. Self-similarity of velocity profiles near the section 4·5 m from the inlet

vegetation strip involved a lot of work, it was a much more favourable procedure than the frequent practice of using artificial plants (e.g. Kubrak *et al.*, 2013). Gramineous weeds were classified into the Poaceae or Gramineae family, is one of the largest vegetation families. The leaves of the gramineae family are long and narrow. Normally, vegetation strips on channel beds are observed only along one side of the river bank at different sites (without vegetation strips on the other side). Therefore, only one side of the laboratory flume bed was covered with a vegetation strip in this study. The degree of submergence of vegetation (the ratio of water depth to vegetation height) was about 2. The planting density was 200 stems/m. The median length and the bend length of the vegetation were 17·4 cm and 7·2 cm, respectively. Each plant had two to four leaf modes on each stem.

The flexibility of vegetation was normal, depending on the flow velocity. In order to have approximately similar vegetation in the flume, the vegetation for the laboratory was collected from the bank of the Kaj River. The lodging velocity was low enough to prevent erosion and was high enough to prevent sediment depot. The average lodging velocity was 0·1 m/s.

The vegetation density a (stems/m) was determined by dividing the projected plant area perpendicular to the flow by the vegetation volume (Nezu and Sanjou, 2008) according to $a = (A/V) = (n\overline{A_i}\,/WhL)$ where n is the number of plants in area $W \times L$ (W is the channel width and L is the channel length), $\overline{A_i}$ is the mean frontal vegetal area and h is the vegetation bending height. To express the vegetation density as a dimensionless factor, the vegetation density was calculated as $\lambda = a \times h$ and, in this study, the dimensionless vegetation density was 0·243.

At each cross-section, measurements were taken for the acquisition of three velocity profiles at distances of 2 cm, 4·5 cm and 7 cm from the vegetation strip (note that 'near the vegetation strip' in this paper refers to distances 2 cm from the vegetation strip). To better understand the effect of non-uniform flow on turbulence characteristics in the presence of a vegetated strip, one experimental run was conducted under the same flow conditions (same flow depth and slope) but without the vegetation strip and another experimental run was conducted under the conditions of uniform flow (zero pressure gradient) without the vegetation strip.

Table 1. Summary of data from laboratory experiments

Case	Distance from inlet: m	Distance from wall: cm	u_{max}: cm/s	u_*: cm/s	H: m	H/d_{50}	Froude number	Re	Remarks
Vegetated bank	5·50	15 (near vegetated bank)	47·87	3·86	0·200	3·81	0·24	$6{\cdot}81 \times 10^4$	$Q = 50$ l/s
		20 (centre)	45·81	2·48	0·200	3·81	0·29	$8{\cdot}24 \times 10^4$	
	6·00	15 (near vegetated bank)	50·59	4·03	0·185	3·52	0·26	$7{\cdot}35 \times 10^4$	$S_0 = -1{\cdot}5\%$
		20 (centre)	48·58	7·58	0·185	3·52	0·24	$6{\cdot}72 \times 10^4$	
	6·50	15 (near vegetated bank)	50·00	4·97	0·182	3·46	0·26	$7{\cdot}16 \times 10^4$	$d_{50} = 0{\cdot}0525$ m
		20 (centre)	55·27	7·35	0·182	3·46	0·28	$7{\cdot}90 \times 10^4$	
	6·75	15 (near vegetated bank)	50·08	5·58	0·180	3·42	0·24	$6{\cdot}62 \times 10^4$	
		20 (centre)	54·63	4·30	0·180	3·42	0·35	$9{\cdot}83 \times 10^4$	
Bare bank	5·50	20 (centre)	43·92	4·55	0·200	3·81	0·21	$5{\cdot}96 \times 10^4$	
	6·00	20 (centre)	54·60	2·24	0·185	3·52	0·34	$9{\cdot}41 \times 10^4$	
	6·50	20 (centre)	47·09	2·05	0·182	3·46	0·31	$8{\cdot}60 \times 10^4$	
	6·76	20 (centre)	55·54	6·24	0·180	3·42	0·31	$8{\cdot}68 \times 10^4$	
Uniform flow	5·50	20 (centre)	63·21	6·40	0·200	3·81	0·26	$7{\cdot}41 \times 10^4$	
	6·00	20 (centre)	63·00	6·86	0·200	3·81	0·24	$6{\cdot}72 \times 10^4$	
	6·50	20 (centre)	53·80	4·17	0·200	3·81	0·27	$7{\cdot}52 \times 10^4$	
	6·76	20 (centre)	53·72	2·93	0·200	3·81	0·30	$8{\cdot}53 \times 10^4$	

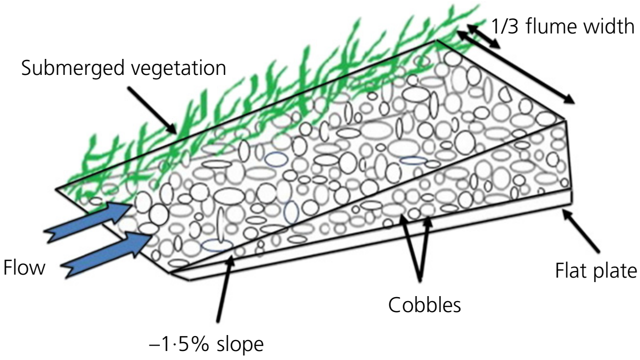

Figure 3. Sketch of vegetation strip and cobble bed under FPG flow

Point velocities were measured in order to obtain velocity profiles in the study reach of the Kaj River. One bank of the studied river reach was vegetated while the other side of the channel was bare. The average water depth of the selected reach was 28 cm, close to that in the laboratory flume. Figure 4(a) shows the selected study reach of the Kaj River.

A down-looking acoustic Doppler velocimeter (ADV), developed by Nortek, was used to measure instantaneous three-dimensional velocity components with a sampling frequency of 200 Hz and a sampling volume of 5·5 mm^3 Figures 4(a) and 4(b). The duration of each measurement was 2 min, acquiring 24 000 instantaneous velocity data for each point. The signal-to-noise ratio (SNR) was recorded in the ADV file and used for assessing the strength of the received acoustic signal against the ambient electronic noise level of the ADV (SonTek, 2002).

(a)

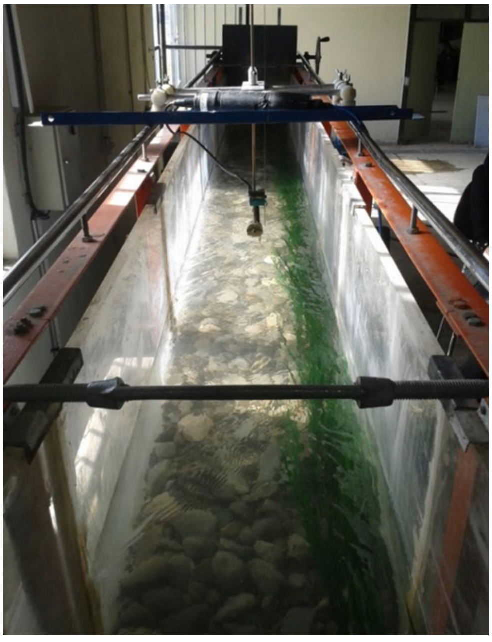

(b)

Figure 4. Use of ADV on cobble bed and vegetation strip in (a) Kaj River and (b) laboratory flume

To obtain high-quality data from the ADV, SNR values should be greater than 5 dB for measurements of mean flow velocity and greater than 15 dB for measurements of instantaneous velocity or turbulence quantities (Garcia *et al.*, 2005). WinADV software was used for data filtering. To assess the quality of the velocity measurements, one of the real-time outputs provided by the ADV is a statistic correlation. This correlation, when used with the SNR, provides an excellent way to manage the quality of ADV measurements. If the average correlation was less than or equal to 70%, the measured velocity data were filtered out. Measurements at a depth of less than 5 cm from the water surface could not be used due to limitations of the ADV. This meant that data were collected from near the bed to the location where the ADV was operational. Different methods were considered for filtering and the filtering method of Goring and Nikora (2002) and Wahl (2002) was selected for this study. This method eliminates less data and leads to good results. For example, when the Goring and Nikora (2002) and Wahl (2002) filtering method is used for shear stress distributions, the calculated bed shear stress shows good agreement with the logarithmic law and the boundary layer characteristics method. All statistical parameters resulting from WinADV, including the SNR and the correlation coefficient, had high values. Using Goring and Nikora's method, it was found that more data were eliminated approaching the water surface. However, a SNR of more than 20, a correlation coefficient of 99% and a similar distribution of data for 120 s and 300 s data collection periods confirmed the accuracy of the results.

Velocity fluctuations in the longitudinal direction (u') and vertical direction (w') were calculated using

2. $$u' = u_\mathrm{i} - u$$
$$w' = w_\mathrm{i} - w$$

where u and w are the time-averaged velocity in longitudinal and vertical directions, respectively, and u_i and w_i are the instantaneous velocities in longitudinal and vertical directions, respectively.

Quadrant analysis was used to assess the characteristics of Reynolds stress. Bursting events are quantified by means of conditional statistics of the velocity fluctuations (Dey, 2014; Dey and Nath, 2010). The hole size parameter H' was defined to distinguish the premier factor ($\overline{-u'w'}$) involved at each quadrant and to bring out u' and w' by increasing the sampling time. The hole size parameter is a hyperbolic region that is a threshold level (Dey and Nath, 2010); $H' = 0$ indicates that the H' curve included every value. By increasing H', weak events gradually disappear and strong events remain (Lu and Willmarth, 1973). According to Yue *et al.* (2007), the detection function (I) is defined as

3. $$I_{(i,H')}(u',\, w') \begin{cases} 1 & \text{if } (u',\, w') \text{ is in quadrant } i \text{ and if} |u'\, w'| \geq H'\, \overline{(u'u')}^{0{\cdot}5}\, \overline{w'w'^{0{\cdot}5}} \\ 0 & \text{otherwise} \end{cases}$$

At any point, the contribution of $\overline{-u'w'}$ from the ith quadrant excluding a hyperbolic hole region of size H' is obtained from (Yue *et al.*, 2007)

4. $$\langle u'w' \rangle_{i,H'} = \lim \frac{1}{T} \int_0^T u'(t) w'(t) I_{i,H'}[u',\, w']\, \mathrm{d}t$$

in which T is the time interval and the square brackets indicate a conditional average, If (u', w') exists in the *ith* quadrant, $I_i = 1$; otherwise, $I_i = 0$.

$S_{i,H'}$ is the contribution of $\overline{-u'w'}$ from each event and can be obtained from

5. $$S_{(i,H')} = \frac{\langle u'w' \rangle_{i,H'}}{u'w'}$$

Based on the sign of the two fluctuating components (u' and w'), four quadrants can be considered ($i = 1$–4) in which

- $i = 1$ represents outward motion ($u' > 0$ and $w' > 0$)
- $i = 2$ represents ejection motion ($u' < 0$ and $w' > 0$)
- $i = 3$ represents inward motion ($u' < 0$ and $w' < 0$)
- $i = 4$ represents sweep motion ($u' > 0$ and $w' < 0$)

Each event is responsible for momentum transport caused by the turbulence. This analysis was applied to examine the contribution of each quadrant to the Reynolds shear stress for FPG flow over a cobbled and vegetated bed. To determine the contribution of each quadrant to the Reynolds stress, a computer program was written in Matlab. The results of the experiments in the laboratory flume and the results based on field surveys of studied river reach are summarised in Tables 1 and 2, respectively. In this study, the values of shear velocity (u_*) for both flume experiments in the laboratory and field measurements in the river were obtained using the boundary layer method (Afzalimehr and Rennie, 2009).

The correlation coefficient between u' and w' was examined by means of $r_{u'w'} = \overline{u'w'}/(u_{\mathrm{rms}} w_{\mathrm{rms}})$, where $\overline{u'w'}$ is the time-averaged value of shear stress and $u_{\mathrm{rms}} = \overline{(u'^2)}^{1/2}$ and

Table 2. Summary of data from the Kaj River

Case	u_{max}: cm/s	u_*: cm/s	H: m	H/d_{50}	Froude number	Re	Remarks
Vegetated bank	36·07	3·98	0·29	7·77	0·14	$6{\cdot}80 \times 10^4$	$d_{50} = 0{\cdot}0373$ m
Bare bank	54·86	6·31	0·28	7·50	0·23	$10{\cdot}80 \times 10^4$	

$w_{rms} = (\overline{w'^2})^{1/2}$ are, respectively, the root mean square of the stream-wise velocity component and the vertical velocity component. The contributions of horizontal and vertical fluctuations on the turbulence process could then be assessed (Schlichting and Gersten, 2000).

3. Results and discussion

3.1 Velocity profiles

Figures 5(a)–5(c) show the distributions of dimensionless velocity at three locations: the central axis of the flume, near the vegetation strip in the flume and the Kaj River, respectively. To better understand the effect of non-uniform flow (FPG) for a vegetated bank or a bare bank, the results are compared with those under uniform flow conditions.

The dip phenomenon (the position at which the maximum velocity appears below the water surface) was not observed for uniform flow (Figure 5(a)). However, for the FPG case, the dip phenomenon occurred for both the FPG with a vegetation strip (Figure 5(b)) and the FPG without a vegetation strip (Figure 5(c)). Wang *et al.* (2015) claim that large-scale roughness often results in an S-shaped velocity profile. The reason for the occurrence of the maximum velocity below the water surface was not due to secondary currents caused by a small aspect ratio ($W/H = 2$, where W is the flume width and H is the water depth) or vegetation, as it was observed in Figure 5 (a) as well as Figures 5(b) and 5(c). The FPG thus has an effect on the occurrence of maximum velocity below the water surface. Graf and Altinakar (1993, 1998) reported that no dip was observed for uniform flow or unfavourable pressure gradient flow.

As shown in Figures 5(b) and 5(c), the velocity regime was divided into either two or three sub-zones with the presence of a submerged vegetation strip in the laboratory flume and the Kaj River. For the case of three sub-zones, in the first sub-zone ($0 \leq z/H \leq 0{\cdot}05$), the velocity remained approximately constant or with a low gradient due to the wake of the vegetation. Ghisalberti and Nepf (2006) adopted the elevation h_1, at which $\overline{u'w'}$ decayed to zero, and called the sub-zone of $0 \leq z \leq h_1$ the 'wake zone'. As shown in Figure 5(b), this sub-zone was thinner than the other sub-zones. Since the application of the ADV was also limited near the channel bed, data from right on the channel bed could not be collected. In the second sub-zone ($0{\cdot}05 \leq z/H \leq 0{\cdot}55$), the velocity profile showed a considerable gradient and an inflection point existed within this sub-zone. Ghisalberti and Nepf (2006) adopted the elevation of h_2, at which $\overline{u'w'}$ again reached zero, and termed this sub-zone ($h_1 \leq z \leq h_2$) the 'mixing layer zone'. As shown in Figure 5(b), the curvature of the velocity profile changed at the inflection point for flows in the channel with a vegetation strip. The third sub-zone ($0{\cdot}55 \leq z/H \leq 0{\cdot}8$), which is called the 'logarithmic zone', is located above the mixing layer. The elevation of h_2 is defined as the elevation of the starting deviation from the universal logarithmic law profile. For the river case (Figure 5(c)), the third sub-zone for flow in the channel without the vegetation strip was not clear. However, for flows in a channel with a vegetation strip, different distributions were found in the three sub-zones, showing an S-shaped distribution in the mixing layer zone.

The log-law velocity distribution is defined as

$$6. \quad \frac{u}{u_*} = \frac{1}{\kappa} \ln\left(\frac{z - d}{z_0}\right)$$

where d is the zero-plane displacement thickness, u_* is the shear velocity, z_0 is the roughness height and κ is the von Karman constant, which is taken 0·41. The value of d is difficult to define, but was determined to be 0·001 m by a trial and error process. The value of z_0 was assumed equal to the value of d_{84} in this study.

Figure 6 shows application of the log law in the logarithmic zone for cross-sections located 5·5 m, 6 m and 6·75 m downstream from the flume entrance. The figure shows that the data deviated from the log law. This may be caused by irregularity of the channel bed due to variable roughness element sizes, the cobble arrangement, bed forms, the interaction of individual roughness elements with flow near the bed (Plott *et al.*, 2013) and very complex interaction of the flow with the vegetation strip. Graf and Altinakar (1993, 1998) claimed that the log law fitted data well for FPG flow in the absence of vegetation in the zone $z/H < 0{\cdot}2$. It may be concluded that, in the course of calculating fluvial hydraulics parameters, application of the log law to determine shear velocity or bed shear stress is not justifiable. Thus, the calculated results may be either considerably overestimated or significantly underestimated.

In this study, the flow above the vegetation followed a logarithmic trend, in agreement with the results reported by Nepf and Ghisalberti (2008), who noted a submerged canopy appearing in the flow as additional roughness and that velocity profiles far above the canopy were logarithmic.

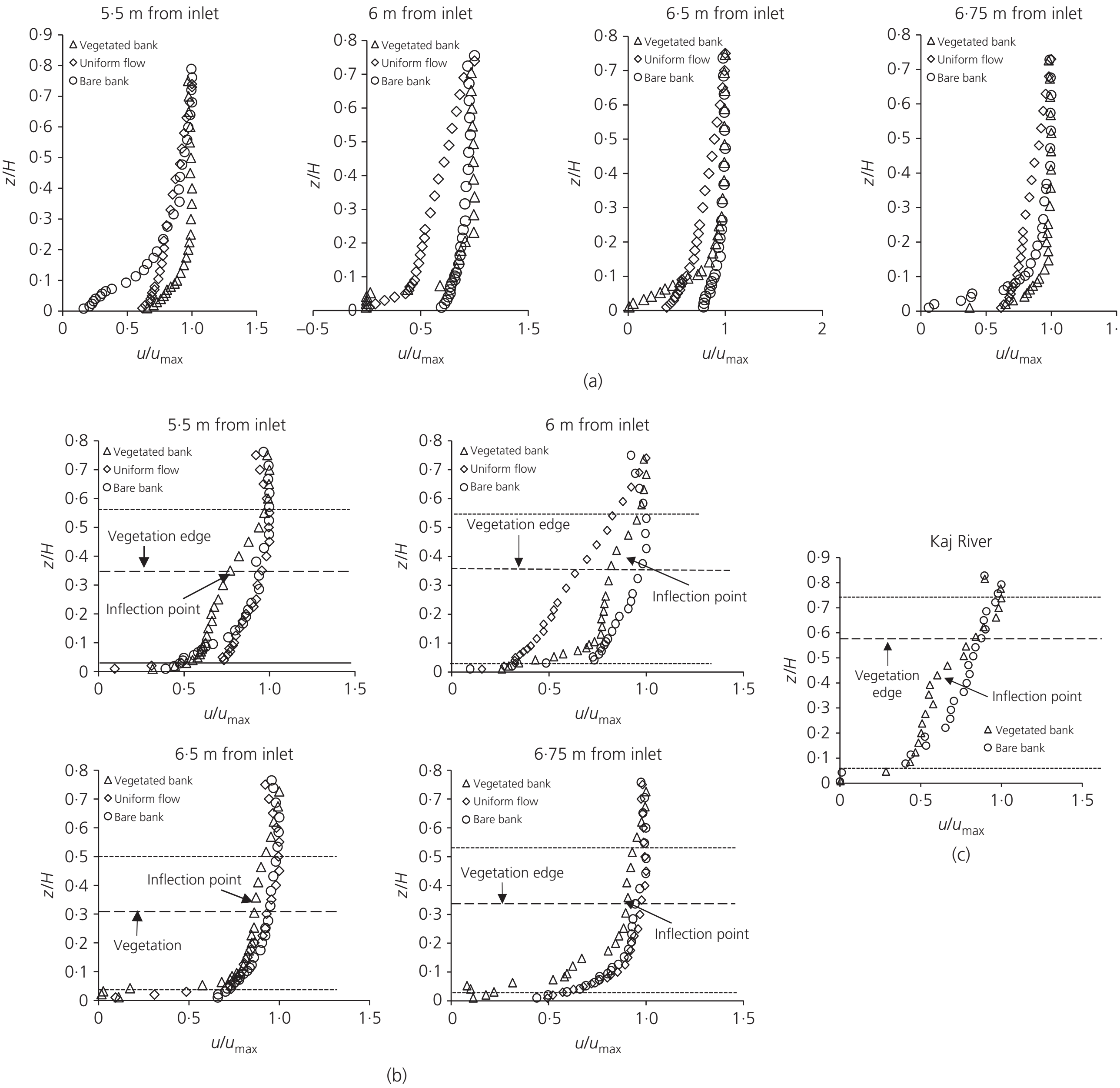

Figure 5. Comparison of dimensionless stream-wise velocity: (a) central axis of the flume; (b) near the vegetation strip in the flume; (c) near the vegetated strip and the bare bank location in Kaj River

3.2 Secondary currents

Secondary currents may be caused by the non-uniformity of flow near the channel boundaries. These induce anisotropic turbulence in which $v'^2 \neq w'^2$. In addition, the variation of grain size across a channel can also generate secondary currents; these are called secondary currents of Prandtl's second kind, which occur in straight channels (Dey, 2014). Secondary currents influence flow characteristics and often cause the dip phenomenon (Leopold, 1994). The term $(v'^2 - w'^2)/u_*^2$ is an indicator for rotational acceleration of a fluid element about the stream-wise axis due to turbulence anisotropy, resulting in secondary currents due to stream-wise vorticity (Dey, 2014; Nezu and Nakagawa, 1993), in which the shear velocity (u_*) is obtained using the boundary layer characteristics method (Afzalimehr and Rennie, 2009). In addition, this term indicates the production of turbulence due to non-uniform distributions of anisotropic Reynolds stress. As discussed by Dey (2014), some researchers have attempted to relate this term to bed shear stress in order to understand the effect of anisotropic turbulence on the Reynolds stress distribution. As shown in Figure 7, in the vicinity of the bed ($z/H < 0{\cdot}05$), $(v'^2 - w'^2)/u_*^2$ increases and then decreases up to the vegetation edge

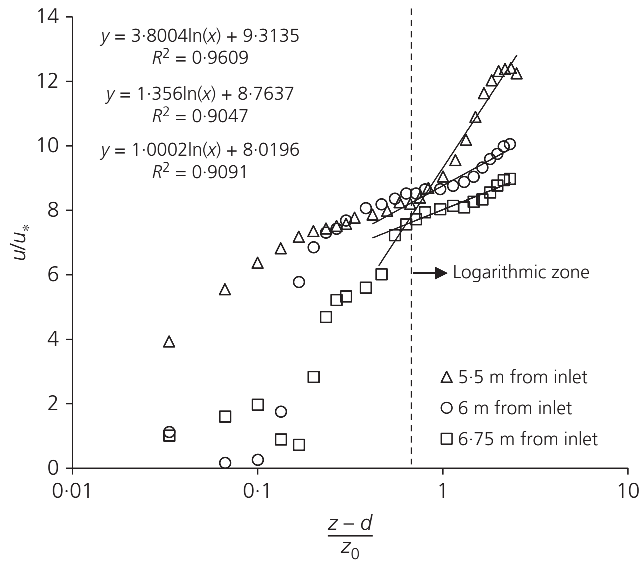

Figure 6. Log-law velocity profiles near the vegetation strip in the flume

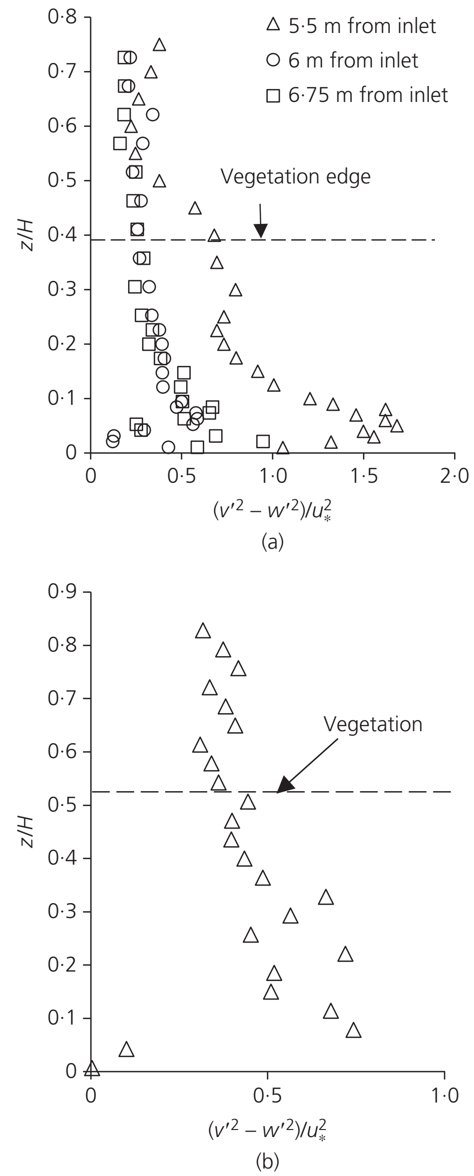

Figure 7. Comparison of dimensionless vorticity parameter near the vegetation strip under non-uniform flow: (a) in the flume; (b) in the Kaj River

(the mixing layer) for FPG flow in both the laboratory (Figure 7(a)) and river (Figure 7(b)) cases. However, the laboratory results of the $v'^2 - w'^2/u_*^2$ patterns in the log-law layer are different from those in the river. The decreasing trend of the vorticity parameter in the log-law layer is due to the dip phenomenon, where du/dz decreases.

The results of the present study under the FPG flow condition were compared with the results reported by Fazlollahi *et al.* (2015), who investigated the impacts of pools and vegetated banks on turbulent flow characteristics under flow with an unfavourable pressure gradient using the same laboratory flume. The comparison revealed that the distributions of the vorticity parameter followed approximately similar patterns, but the Reynolds stress distributions obtained in the present study were different from those reported by Fazlollahi *et al.* (2015). As shown in Figure 8, based on the data collected from both the laboratory flume and the Kaj River, there was no relation between the vorticity parameter and the Reynolds stress distributions.

3.3 Reynolds stress

Reynolds shear stress ($-\rho\overline{u'w'}$) is an important parameter in the understanding of turbulence in which ρ is mass density of water. Because Reynolds shear stress controls the rate at which sediment is re-entrained from the bed, it plays a decisive role in sediment transport processes and open-channel stability (Lopez and Garcia, 1998). Either the horizontal momentum flux in the vertical direction or the vertical momentum flux in the horizontal direction can be represented by the term ($-\rho\,\overline{u'w'}$). As illustrated in Figure 8, the values of Reynolds stress were normalised by the square of shear velocity (u_*^2). The flow separation around cobble particles and secondary currents due to different grain size affect the shear stress distributions and thus led to data scatter near the channel bed. A number of negative values of Reynolds shear stress were found near water surface, especially under non-uniform flow conditions. For a channel without vegetation, the classic Reynolds stress equation ($\partial p/\partial x = \partial\tau/\partial z$) can be used to interpret the patterns. Accordingly, in FPG flow, the pressure gradient was negative, making the vertical distribution of Reynolds stress to become negative. Therefore, the Reynolds stress decreased towards the water surface with a concave distribution trend. In addition, for the uniform flow, a non-linear distribution ($\tau = \gamma H S_0$) (τ is the Reynolds stress, γ is the specific

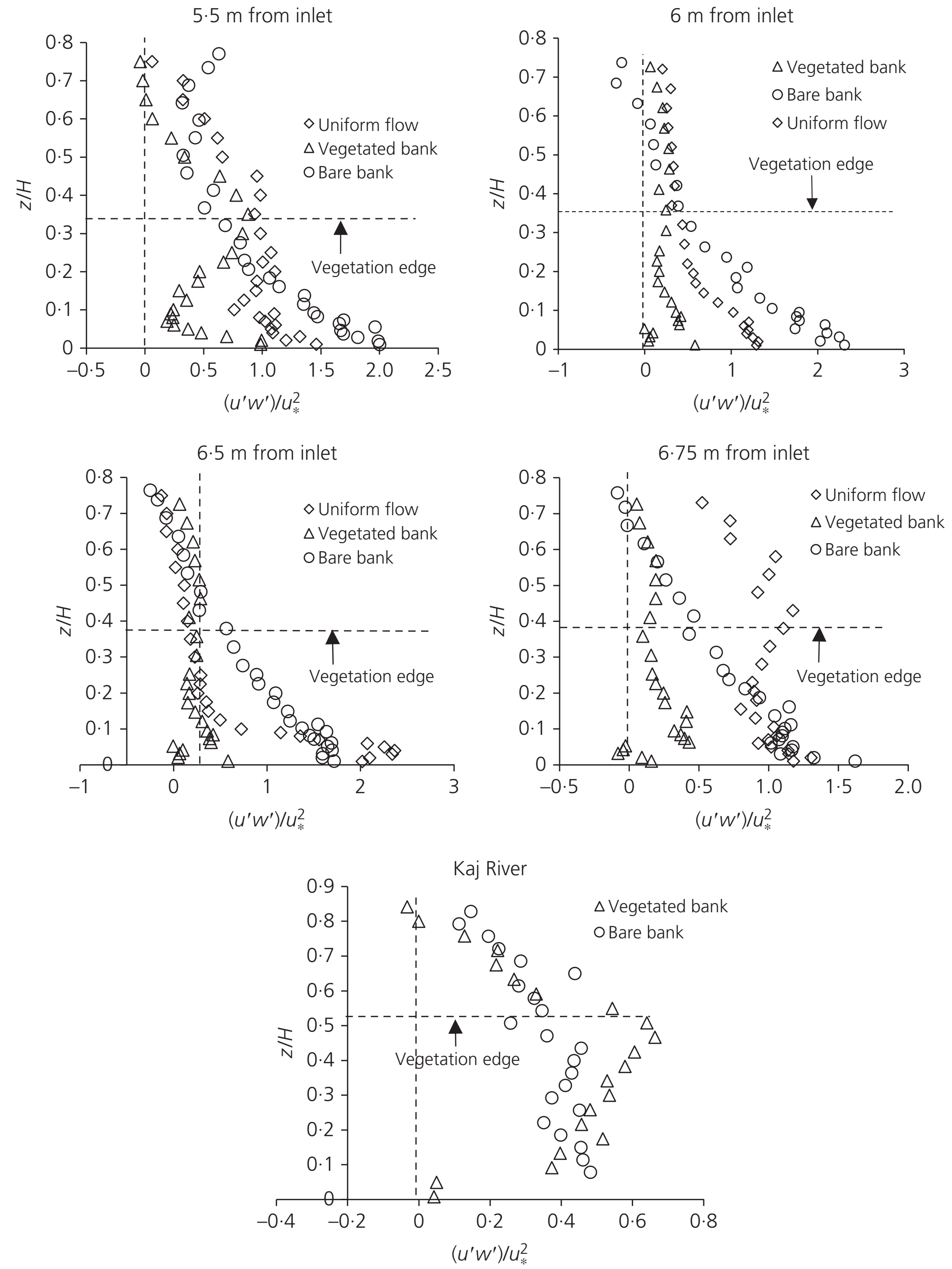

Figure 8. Comparison of dimensionless shear stress distributions under the condition of FPG flow and uniform flow strip in the flume with vegetation strip and without vegetation

weight of water, H is the flow depth and S_0 is the bed slope) was noted, due to anisotropic turbulence generated by the coarse bed and the vegetation strip.

The distribution of Reynolds stress for flow with a vegetated strip showed either a two-layer pattern or a three-layer pattern. For the three-layer case, the laboratory measurements revealed a decreasing trend from the channel bed to a flow depth of $z/H = 0{\cdot}1$, an increasing trend from $z/H = 0{\cdot}1$ to $z/H = 0{\cdot}35$ and then again a decreasing trend towards the water surface (a Z-shaped Reynolds stress distribution). However, for the three-layer case based on measurements from the Kaj River, an increasing trend was observed in the mixing layer, which was independent of the effect of the vegetation strip. This may be due to a difference in the size of eddies and vortices in the natural river from those in the laboratory. The maximum

Reynolds stress occurred in the mixing layer over the vegetation strip ($z/H = 0{\cdot}5$) for the river case, but near the channel bed for the laboratory case.

3.4 Quadrant analysis

Quadrant analysis was to investigate the effect of a vegetated strip over a cobble bed on the characteristics of non-uniform flow. The results indicated that sweep and ejection turn out to be the most dominant events near the vegetation strip. This finding is similar to the results from previous research projects using vegetated channel banks instead of a vegetation strip on a channel bed (Afzalimehr *et al*., 2012, 2015; Fazel *et al*., 2015; Franca *et al*., 2014). Yue *et al*. (2007) pointed out that sweep motions were the major contribution to Reynolds stress within the vegetation. Figure 9(a) shows the frequency of occurrence of all kinds of events as a function of normalised distance from the channel bed at the central axis of flume in the presence of a vegetation strip. The dominance of sweeps over ejections, outward and inward interactions are obvious from the bed to near the water surface. However, near the water surface, outward interactions were the most dominant events. Figure 9(b) shows the ratio of sweeps to ejections near

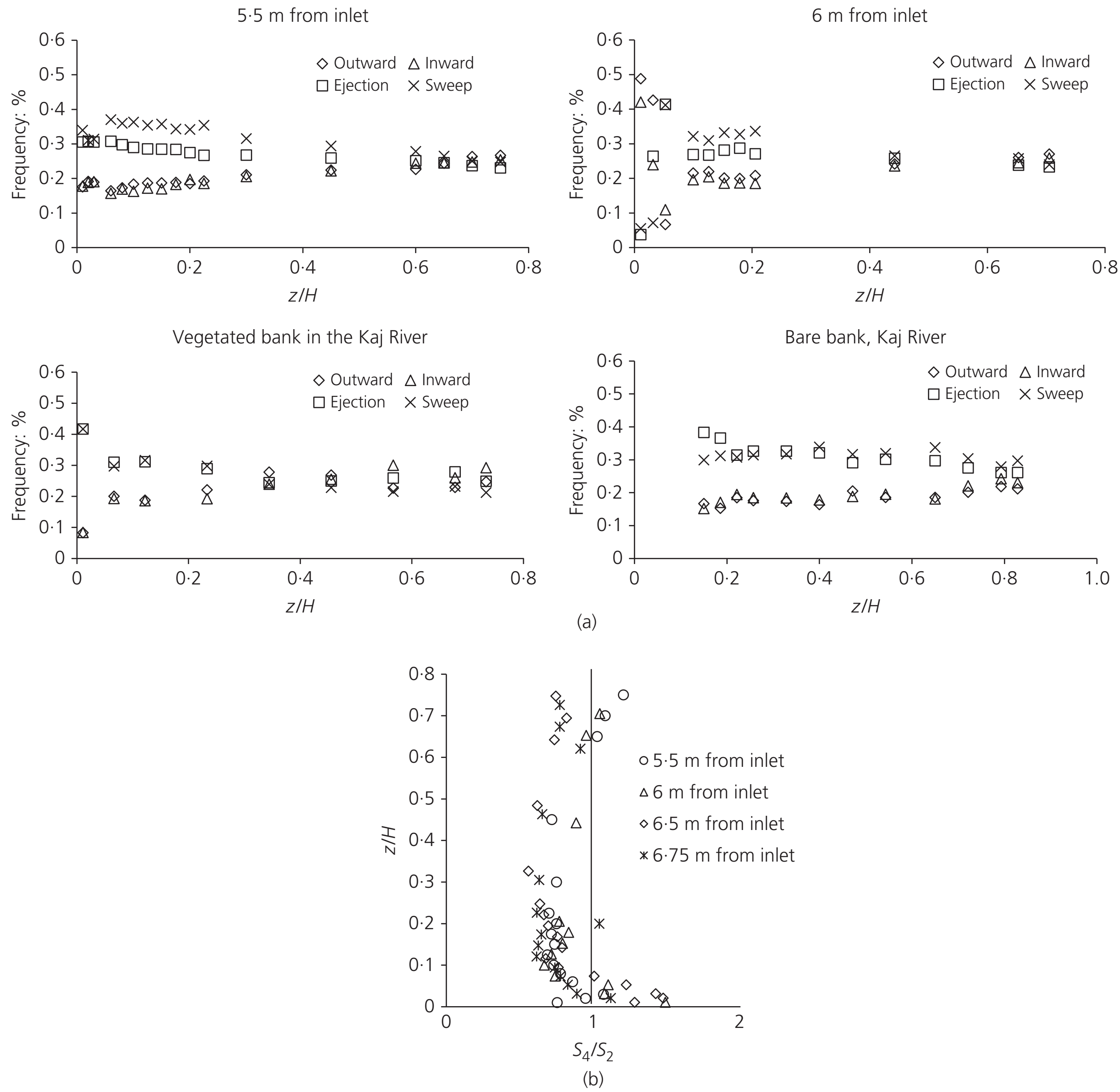

Figure 9. (a) Frequency of velocity fluctuations in longitudinal direction (u') and vertical direction (w') for each quadrant ($i = 1$–4) under FPG flow in the flume with a vegetation strip at cross-sections of 5·5 m, 6 m, 6·5 m and 6·75 m from inlet. (b) Ratio of sweeps to ejections under FPG flow in flume with vegetation strip at cross-sections of 5·5 m, 6 m, 6·5 m and 6·75 m from inlet

the vegetation strip. As shown in Figure 9, in the zone from the channel bed to a depth of $z/H = 0{\cdot}25$, sweep motions were more frequent than ejection events. This means that sweep motion is responsible for momentum transport from the water body over the vegetation towards the vegetated region near the channel bed.

The maximum value of the sweep to ejection ratio was 1·65. This ratio was about 0·8 from a water depth of $z/H = 0{\cdot}25$ towards the water surface, which is in good agreement with results reported by Yue *et al*. (2007). Using the large eddy simulation method, Yue *et al*. (2007) found a ratio of 2 within the plant canopy region. Dey (2014) claimed that both sweeps and ejections significantly affect Reynolds stress production, while both outward and inward events play a weaker role near the bed, confirming the dominant contribution of sweep and ejection for momentum transfer towards the bed region. Similar patterns in the laboratory and river were found for different events, as shown in Figure 9(a).

According to Figure 9, from the bed to the top of the canopy, sweep and ejection were the most frequent events, while outward and inward events contributions were more significant from the vegetation edge up to the water surface. This trend shows that the momentum transfer between the flow and the vegetated channel bed was mostly due to sweep and ejection events while outward and inward events have a significant effect on Reynolds stress near the water surface.

Figure 10 shows the sum of the four quadrant fractions plotted against hole size parameter at different elevations from the bed close to the vegetation. A change in hole size parameter from 0 to 1 had no influence on the stress fraction. As expected, an increase in hole size parameter led to a decrease in the sum of the four quadrant fractions expect for a flow depth of $z/H = 0{\cdot}7$ at a cross-section 5·5 m downstream from the flume entrance. In the presence of the vegetation strip, a change in hole size parameter led to a more rapid decrease in the stress fraction close to the channel bed ($z/H = 0{\cdot}03$ and $z/H = 0{\cdot}08$) compared with that near the water surface ($z/H = 0{\cdot}70$).

3.5 Momentum transport

The correlation coefficient $r_{u'w'}$ is an indicator to assess changes in the efficiency of turbulence in momentum

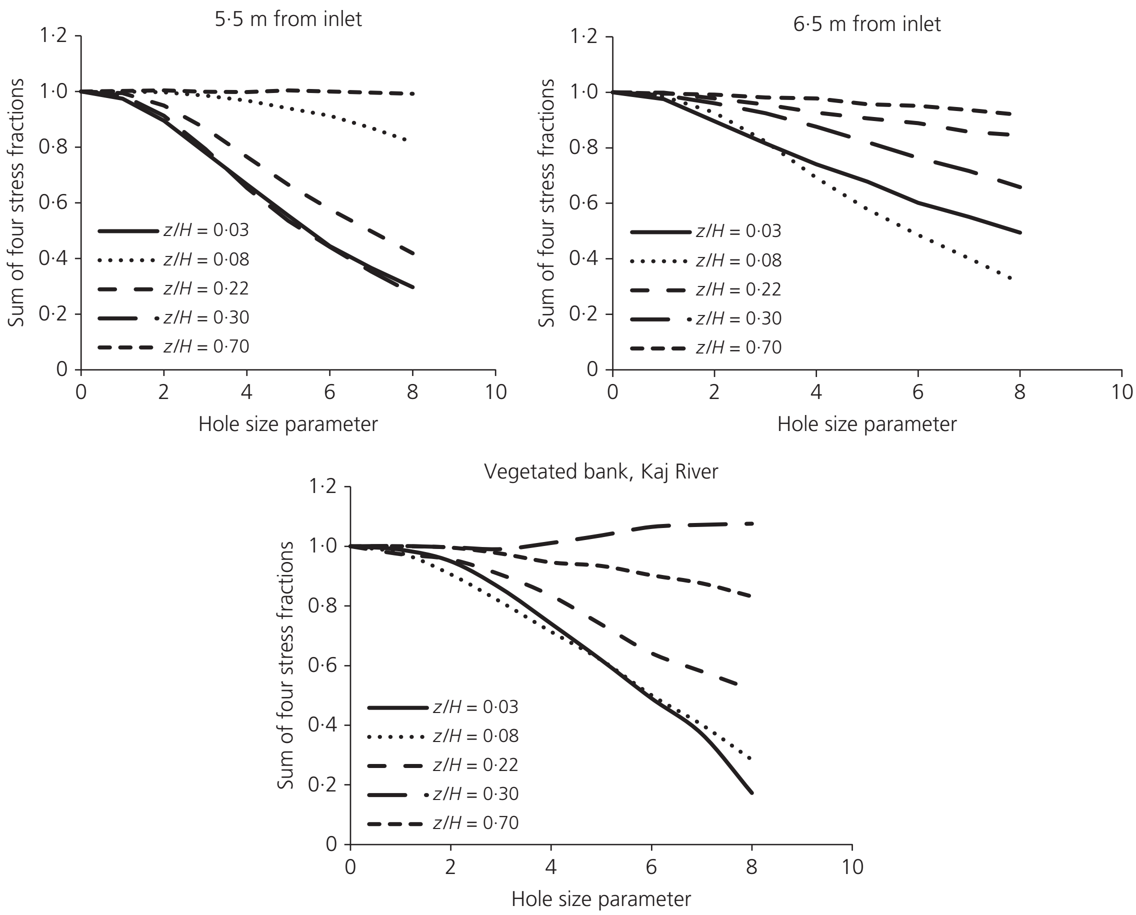

Figure 10. Sum of all four quadrant fractions plotted against hole size parameter near vegetated strip at cross-sections of 5.5 m, 6 m, 6.5 m and 6.75 m from inlet

transport. A change in both the sign and magnitude of $r_{u'w'}$ means that there is a dominant change in the anisotropy of turbulence. As shown in Figure 11, the change in magnitude of $r_{u'w'}$ for the channel with a vegetation strip was greater than that for the channel without vegetation. In addition, the change in magnitude of $r_{u'w'}$ was more than that under uniform flow conditions.

The magnitude of $r_{u'w'}$ under the uniform flow condition was approximately constant and negative over the whole flow depth, and no significant changes in momentum transport were observed. Negative values of $r_{u'w'}$ from the bed to $z/H = 0{\cdot}6$ indicate that ejection and sweep motions in a bursting process were significantly correlated. Positive $r_{u'w'}$ values from $z/H = 0{\cdot}6$ to the water surface indicate that outward and inward interactions correlate more frequently at the bare bank and the vegetated bank under FPG. A change in the sign of $r_{u'w'}$ indicates that there is a change in the direction of momentum transport, whereas a change in the magnitude of $r_{u'w'}$ indicates a change in the efficiency of the turbulence to transport momentum (Kaimal and Finnigan, 1994). In addition, a negative value of $r_{u'w'}$ reveals the dominance of sweep and ejection events in bursting cycles and downward momentum transport. However, the correlation coefficient tended to be positive near the water surface, meaning that turbulence was due to upward momentum transport near the water surface. Figure 11 reveals a difference in momentum transport in the laboratory flume and in the Kaj River. The magnitude of $r_{u'w'}$ under uniform flow conditions was approximately constant over the whole flow depth and no significant changes in momentum transport have been observed. As shown in Figure 11, the value of $-r_{u'w'}$ near the top of the vegetation under FPG flow was about 0·15 to 0·30. Raupach *et al*. (1996) also calculated the value of $-r_{u'w'}$ and found it to vary from 0·40 to 0·60 near the top of the canopy (in the canopy mixing layer) in terrestrial submerged canopies under uniform flow conditions. Ghisalberti and Nepf (2002) carried out experiments in a flume with aquatic vegetation canopies and found that $-r_{u'w'}$ was around 0·5 near the top of the canopy in the canopy mixing layer.

4. Conclusions

Reported research into the interaction of submerged vegetation and non-uniform flow is limited. However, how this interaction may affect the estimation of the main hydraulic parameters (e.g. roughness coefficient) is of interest to managers and engineers. For research in this area, it may be very difficult to take into account scale effects, but as similar as possible conditions between river and laboratory were considered in this study. The authors walked more than 10 km to find flow conditions without the occurrence of either erosion or sediment deposition. It is very complex task to scale a river in a laboratory because many uncontrolled variations play a significant role in flow structures. Also, the aim of the work was not to model the river in the laboratory, but to explore the hydrodynamic implications of the presence of a submerged vegetation strip on a cobble bed under non-uniform flow in both the laboratory and field. The width and water depth at the selected site in the Kaj River were 8 m and 28 cm, respectively. Had the river been modelled in the laboratory, the particles would have been sand size and the flow depth would have been 0·6 cm, changing turbulent flow in the river into laminar sheet flow in the laboratory. A reach with minimum bed forms, the fewest cross-section changes and with vegetation cover on one side demands considerable work, time and funding. This is especially true in rivers with cobble beds where changes in river morphology and bed material are often observed. In addition, in this study, the relative submergence (H/d_{50}) (H is flow depth and d_{50} is the median grain size) were selected such that the applied laws (e.g. the log law) remained valid for both river and laboratory conditions.

Decreasing water resources and increasing populations require improved restoration and management in open channels and rivers. It is often assumed that flow is uniform in water resources projects, but a change in bed form and cross-section alters the flow velocity, generating non-uniform flows and affecting resistance to flow and sediment transport estimations. Afzalimehr and Levesque (1999) reported that there is 500% difference in estimation of the Manning coefficient when uniform flow is used rather than non-uniform flow. To understand these huge differences, one needs to consider details in flow structures by using advanced methods such as quadrant analysis for the bursting process. The bursting process, with sweep and ejection events, reveals the contribution of turbulence to the Reynolds stress distribution. An estimation of Reynolds stress allows calculation of the shear velocity and then evaluation of the roughness coefficient. Such an estimation allows one to determine the relation between flow variation and resistance to flow, allowing better decisions to be made and decreasing project costs.

In the present study, the effect of non-uniform flow (FPG) over a cobble bed with a vegetated strip on turbulence characteristics was investigated in both a laboratory flume and an actual river. The following important results were obtained from this study.

(*a*) The presence of submerged vegetation in both the laboratory flume and the river caused the flow velocity profiles to have either two or three sub-zones under flow conditions with a FPG. The dip phenomenon was found to depend on the pressure gradient rather than vegetation strip.
(*b*) Application of the log law for flow with a FPG in a channel with a vegetation strip is not suitable and may lead to considerable errors in the determination of fluvial hydraulic parameters.
(*c*) The vorticity parameter did not affect the Reynolds stress distribution and its distribution was almost independent from the longitudinal pressure gradient.

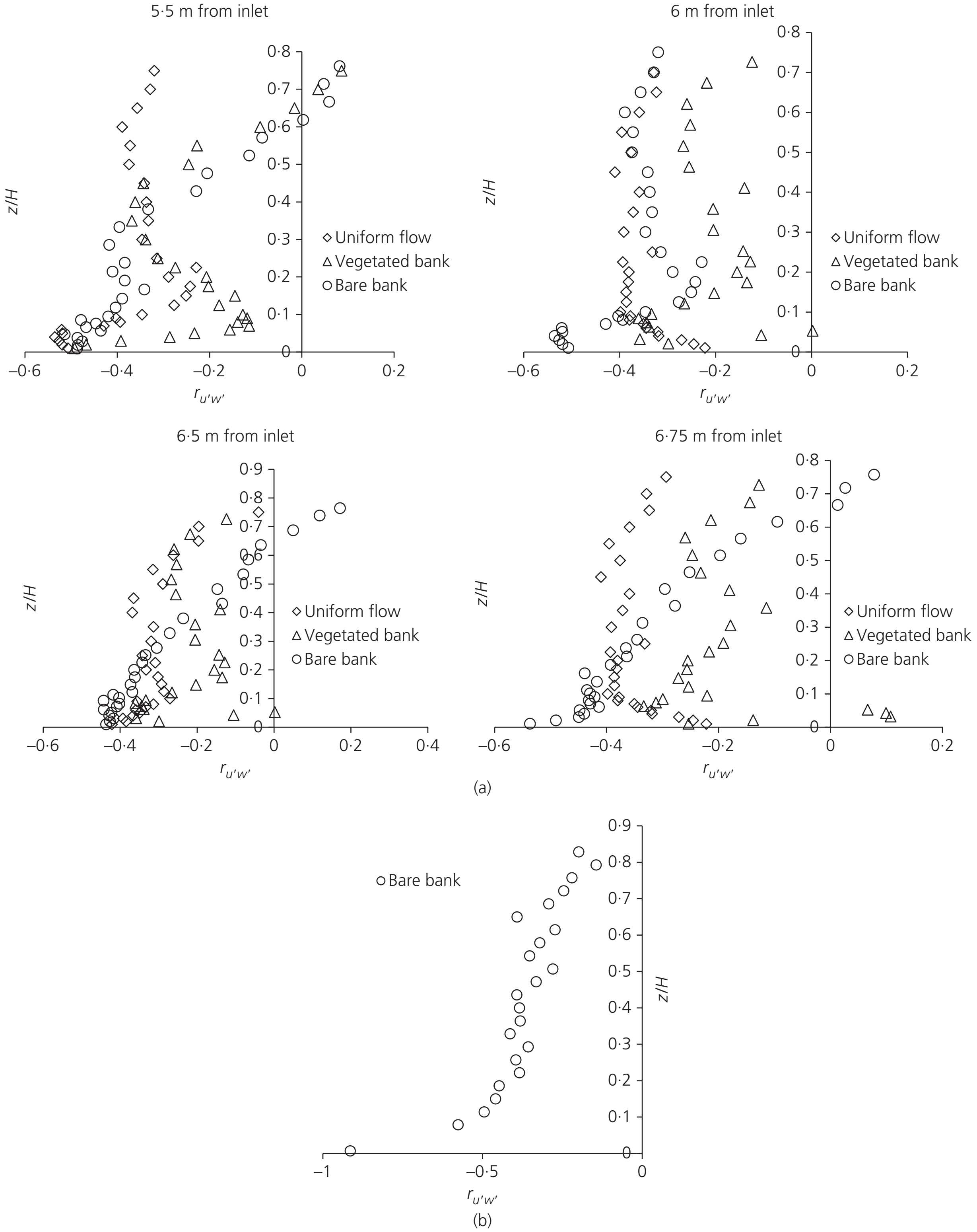

Figure 11. Correlation coefficient ($r_{u'w'}$) between longitudinal fluctuations (u') and vertical fluctuations (w'): (a) vegetation strip, bare bank and uniform flow in laboratory flume; (b) bare bank in the Kaj River

(*d*) Since the turbulent flow structures in the laboratory flume and the Kaj River were different, different Reynolds stress distributions were obtained, especially in the mixing layer zone. This may be attributed to differences in eddy size and vortices in the laboratory flume and in the natural river. The trend of the Reynolds stress distribution in the mixing layer zone was found to be independent of the vegetation strip, showing a similar trend to flow in the channel without vegetation.

(*e*) Interestingly, in the zone from the channel bed to a flow depth of $z/H = 0{\cdot}25$, sweep motions were more frequent than ejection events, showing that sweep is responsible for the transport of momentum from the water surface towards the bed region. The maximum value of the ratio of sweep to ejection motions was 1·65. This ratio was about 0·8 from the depth of $z/H = 0{\cdot}25$ to the water surface, in good agreement with result reported by Yue *et al*. (2007). The results from both the laboratory flume and the natural river showed similar patterns for different quadrants.

(*f*) A negative value of $r_{u'w'}$ reveals the dominance of sweep and ejection events in the bursting cycle and downward momentum transport. However, this correlation coefficient tended to be positive near the water surface. This means that turbulence was due to upward momentum transport near the water surface. The magnitude of $-r_{u'w'}$ under uniform flow conditions was approximately constant over the whole flow depth and no significant changes in momentum transport were observed. The value of $-r_{u'w'}$ near the top of the vegetation under FPG flow was about 0·15 to 0·30. The frequencies of occurrence of sweeps and ejections were higher than those other events, particularly close to the bed.

REFERENCES

Aberle J and Järvelä J (2015) Hydrodynamics of vegetated channels. In *Rivers – Physical, Fluvial and Environmental Processes* (Rowinski P and Radecki-Pawlik A (eds)). Springer International Publishing, Cham, Switzerland, vol. 21, pp. 519–541.

Afzalimehr H (2010) Effect of non-uniformity of flow on velocity and turbulence intensities in flow over a cobble-bed. *Journal of Hydrological Process* **24(3)**: 331–341.

Afzalimehr H and Levesque B (1999) Discussion on friction slope in depth averaged flow. *Journal of Hydraulic Engineering ASCE* **125(5)**: 549.

Afzalimehr H and Rennie CD (2009) Determination of bed shear stress using boundary layer parameters in a gravel-bed river. *Hydrological Sciences Journal* **54(1)**: 147–159.

Afzalimehr H, Fazel E and Singh VJ (2010) Effect of vegetation on banks on distributions of velocity and Reynolds stress under accelerating flow. *Journal of Hydrologic Engineering ASCE* **15(9)**: 708–713.

Afzalimehr H, Fazel E and Ghalichand J (2012) Effects of accelerating and decelerating flows in a channel with vegetated banks and gravel bed. *International Journal of Sediment Research* **27(2)**: 188–200.

Afzalimehr H, Bagheri E, Gallichand J and Dufresne L (2014) Cobble-bed concentration and vegetated banks effects on flow. *Journal of Water Management* **167(4)**: 206–218.

Afzalimehr H, Moradian M, Gallichand J and Sui J (2015) Effect of adverse pressure gradient and different vegetated banks on flow. *River Research and Applications* **32(5)**: 1059–1070.

Choi SUK and Kang H (2006) Numerical investigations of mean flow and turbulence structures of partly-vegetated open-channel flows using the Reynolds stress model. *Journal of Hydrology Research* **44(2)**: 203–217.

Dey S (2014) *Fluvial Hydrodynamics: Hydrodynamic and Sediment Transport Phenomena*. Springer, Berlin, Germany.

Dey S and Das R (2012) Gravel-bed hydrodynamics: a double-averaging approach. *Journal of Hydrologic Engineering ASCE* **138(8)**: 707–725.

Dey S and Nath T (2010) Turbulence characteristics in flows subjected to boundary injection and suction. *Journal of Engineering Mechanics* **136(7)**: 877–888.

Fazel E, Afzalimehr H and Sui J (2015) Turbulence characteristics of favorable pressure gradient flows in gravel-bed channel with vegetated walls. *Journal of Hydrology and Hydromechanics* **63(2)**: 154–163.

Fazlollahi A, Afzalimehr H and Sui J (2015) Impacts of pool and vegetated banks on turbulent flow characteristics. *Canadian Journal of Civil Engineering* **42(12)**: 979–986.

Finnigan J (2000) Turbulence in plant canopies. *Annual Review of Fluid Mechanics* **32(1)**: 519–571.

Franca MJ and Brocchini M (2015) Turbulence in rivers. In *Rivers – Physical, Fluvial and Environmental Processes* (Rowinski PM and Radecki-Pawlik A (eds)). Springer, Cham, Switzerland, pp. 51–78.

Franca MJ, Santos BO, Antico F and Ferreira RML (2014) Quadrant analysis of shear events in open channel flows over mobile and immobile hydraulically rough beds. *ERCOFTAC Bulletin 100*, pp. 29–36.

Garcia CM, Cantero MI, Nino Y and Garcia MH (2005) Turbulence measurements with acoustic Doppler velocimeters. *Journal of Hydraulic Engineering ASCE* **131(12)**: 1062–1073.

Ghisalberti M and Nepf H (2002) Mixing layers and coherent structures in vegetated aquatic flows. *Journal of Geophysical Research* **107(C2)**: 3-1–3-11.

Ghisalberti M and Nepf H (2006) The structure of the shear layer in flows over rigid and flexible canopies. *Journal of Environmental Fluid Mechanics* **6(3)**: 277–301.

Goring DG and Nikora VI (2002) Despiking acoustic Doppler velocimeter data. *Journal of Hydraulic Engineering ASCE* **128(1)**: 117–126.

Graf WH and Altinakar MS (1993) *Hydraulique Fluvial. Volume 1*. Presses Polytechniques et Universitaires Romandes, Lausanne, Switzerland.

Graf WH and Altinakar MS (1998) *Fluvial Hydraulics, Flow and Transport Processes in Channels of Simple Geometry*. Wiley, New York, NY, USA.

Huai WX, Zeng YH, Xu ZG and Yang ZH (2008) Three-layer model for vertical velocity distribution in open channel flow with submerged rigid vegetation. *Advances in Water Resources* **32(4)**: 487–492.

Kaimal J C and Finnigan J (1994) *Atmospheric Boundary Layer Flows: Their Structure and Measurement*. Oxford University Press, Oxford, USA.

Kubrak E, Kubrak J and Rowinski PM (2013) Application of one-dimensional model to calculate water velocity distributions over elastic elements simulating Canadian waterweed plants (Elodea Canadensis). *Acta Geophysica* **61(1)**: 194–210.

Kubrak E, Kubrak J and Kiczko A (2015) Experimental investigation of kinetic energy and momentum coefficients in regular channels with stiff and flexible elements simulating submerged vegetation. *Acta Geophysica* **63(5)**: 1405–1422.

Leopold LB (1994) *A View of the River*. Harvard University Press, Cambridge, MA, USA.

Lopez F and Garcia M (1998) Open-channel flow through simulated vegetation: suspended sediment transport modeling. *Water Resources Research* **34(9)**: 2341–2352.

Lopez F and Garcia M (2001) Mean flow and turbulence structure of open-channel flow through non-emergent vegetation. *Journal of Hydraulic Research* **127(5)**: 392–402.

Lu S and Willmarth W (1973) Measurements of the structure of the Reynolds stress in a turbulent boundary layer. *Journal of Fluid Mechanics* **60(3)**: 481–511.

Maddahi MR, Afzalimehr H and Rowinski PM (2016) Flow characteristics over a gravel bedform: Kaj River case study. *Acta Geophysica* **64(5)**: 1779–1796.

Mrokowska M, Rowinski PM and Kalinowska MB (2015a) Evaluation of friction velocity in unsteady flow experiments. *Journal of Hydraulic Research IAHR* **53(5)**: 659–669.

Mrokowska M, Rowinski PM and Kalinowska MB (2015b) A methodological approach of estimating of resistance to flow under unsteady flow conditions. *Hydrology and Earth System Science* **19**: 4041–4053, http://dx.doi.org/10.5194/hess-19-4041-2015.

Nepf HM and Ghisalberti M (2008) Flow and transport in channels with submerged vegetation. *Acta Geophysica* **56(3)**: 753–777.

Nezu I and Nakagawa H (1993) *IAHR Monograph: Turbulence in Open-Channel Flows*. Balkema, Rotterdam, the Netherlands.

Nezu I and Sanjou M (2008) Turbulence structure and coherent motion in vegetated open-channel flows. *Journal of Hydro-Environment Research* **2(2)**: 62–90.

Okamoto T and Nezu I (2009) Turbulence structure and 'Monami' phenomena in flexible vegetated open-channel flows. *Journal Hydraulic Research* **47(6)**: 798–810.

Plott JR, Diplas P, Kozarek J *et al.* (2013) A generalized log-law formulation for a wide range of boundary roughness typically encountered in natural streams. *Journal of Geophysical Research Earth Surface* **118(3)**: 1419–1431.

Raupach MR, Finnigan JJ and Brunet Y (1996) Coherent eddies and turbulence in vegetation canopies: the mixing-layer analogy. *Boundary Layer Meteorology* **78(3–4)**: 351–382.

Schlichting H and Gersten K (2000) *Boundary Layer Meteorology*, 8 edn. Springer-Verlag, Berlin, Heidelberg, Germany.

SonTek (2002) *SonTek/YSI ADV Field Software Manual*. SonTEK/YSI Inc., San Diego, CA, USA.

Wahl TL (2002) Discussion of "despiking acoustic Doppler velocimeter data" by Derek G. Goring and Vladimir I. Nikora. *Journal of Hydraulic Engineering ASCE* **129(6)**: 484–489.

Wang XK, Chen Y, Wang BJ and Yan XF (2015) Experimental study on velocity profiles with different roughness elements in a flume. *Acta Geophysica Sinica* **63(6)**: 1685–1705.

Wolman MG (1954) A method of sampling coarse river bed material. *Transactions of the American Geophysical Union* **35(6)**: 951–956.

Yue W, Meneveau C, Parlange MB *et al.* (2007) A comparative quadrant analysis of turbulence in a plant canopy. *Water Resources Research* **43(5)**: W05422.

How can you contribute?

To discuss this paper, please email up to 500 words to the editor at journals@ice.org.uk. Your contribution will be forwarded to the author(s) for a reply and, if considered appropriate by the editorial board, it will be published as discussion in a future issue of the journal.

Proceedings journals rely entirely on contributions from the civil engineering profession (and allied disciplines). Information about how to submit your paper online is available at www.icevirtuallibrary.com/page/authors, where you will also find detailed author guidelines.